Honda Research Institute EU
Honda Research Institute Europe GmbH
https://www.honda-ri.de/

Continuous Risk Measures for Driving Support

Julian Eggert, Tim Puphal

2018

Preprint:

This is an accepted article published in International Journal of Automotive Engineering. The final authenticated version is available online at: https://doi.org/[DOI not available]

Continuous Risk Measures for Driving Support

Julian Eggert[1)] Tim Puphal[1)]

1) Honda Research Institute (HRI) Europe
Carl-Legien-Str. 30, 63073 Offenbach, Germany (e-mail:[julian.eggert, tim.puphal]@honda-ri.de)

Received on November 17, 2017

ABSTRACT: In this paper, we compare three different model-based risk measures by evaluating their stengths and weaknesses qualitatively and testing them quantitatively on a set of real longitudinal and intersection scenarios. We start with the traditional heuristic Time-To-Collision (TTC), which we extend towards 2D operation and non-crash cases to retrieve the Time-To-Closest-Encounter (TTCE). The second risk measure models position uncertainty with a Gaussian distribution and uses spatial occupancy probabilities for collision risks. We then derive a novel risk measure based on the statistics of sparse critical events and so-called "survival" conditions. The resulting survival analysis shows to have an earlier detection time of crashes and less false positive detections in near-crash and non-crash cases supported by its solid theoretical grounding. It can be seen as a generalization of TTCE and the Gaussian method which is suitable for the validation of ADAS and AD.

KEY WORDS: **Safety**, Risk Indicators, 2D Risk Measures, Risk Measures, Predictive Risk, Prediction Uncertainty, TTX, Time-To-Collision, TTC, Gaussian Collision Probability, Statistics of Sparse Events, Inhomogenous Poisson Processes, Survival Function, VI-DAS [C1]

1. Introduction

Current progress in the development of Advanced Driver Assistance Systems (ADAS) and Autonomous Driving (AD) is based on a broad range of technological and methodological advances in the field of artificial intelligence. One objective of future ADAS and AD is the improvement of road safety by foreseeing dangerous situations and supporting the driver to behave in an appropriate way mitigating accidents. A key component is therefore the capability of situation risk assessment. Risk is usually defined as the likelihood that a critical event might occur weighted by its probable severity, i.e. its potential consequences in terms of damage, costs and injuries [(1)]. The main problem with risk estimation is its predictive character involving uncertainties (in sensor measurements, driver behavior and scene evolution), which spread over time and which have to be modeled in a sensible way.

In previous related work, numerous approaches for prediction and risk assessment have been introduced [(2)]. On the one hand, it is possible to calculate risks by detecting hazardous driver intentions. For example, the typical steering behavior is learnable using image streams in a with convolutional neural networks [(3)]. Comparing the measured with the learned wheel angle, the deviation can be assumed to correlate to the current risk. Since only the road structure influences the nominal behavior, the resulting risk value indicates curve risk and not collision risk. As an alternative, a Bayesian network [(4)] is employed to classify behaviors into typical maneuvers, e.g. drive straight or turn. Training the network with accident data would lead to maneuver detections of vehicles violating traffic rules. Hereby, risks cannot be identified for situations which are not in the dataset.

On the other hand, risk measures are based on future vehicle trajectories. The Time-To-Collision (TTC) [(5)], as one example of Time-To-Event (TTX) indicators, is defined as the deterministic time until the trajectories of two vehicles intersect. For the trajectory prediction, a constant velocity model is implicitly given in the respective equations. Variants of TTC incorporate different velocity profiles, such as constant acceleration models [(6)]. Since TTC only works for longitudinal scenarios, its equations have been extended for 2D operation [(7)]. Additionally, to overcome the collision assumption in TTC and thus having realistic values in non-crash scenarios the orientation of the vehicles are taken into account. Both drawbacks of TTC are also handled directly with the Time-To-Closest-Encounter (TTCE) [(8)].

Probabilistic risk prediction presumes critical events to act in a defined probability distribution. Gaussian methods [(9)] model a normal distribution for the positions in the predicted trajectories and calculate the collision probability by estimating their overlap. Furthermore to improve the accuracy, the distribution variances are separated into longitudinal and lateral components and instead of integrating analytically, Monte Carlo simulation gives an approximation of the overlap [(10)]. Similarly, the concept of Kamms circle [(11)] is used as positional uncertainty to derive a "Worst-TTC" as the maximal risk value. With Poisson processes [(12)] the probability to remain accident-free can be calculated out of the mean time between critical events, which is dependent on the distances of the future trajectories. The risk measure follows as the complement of the corresponding survival function and allows to consider not only collision risk, but also for instance the risk for losing control in curves.

Despite these works, a theoretically grounded, generalizable, yet efficient risk measure for ADAS and AD is still missing. Risks on the behavioral level [(3,4)] are based on machine learning algorithms and their accuracy is highly influenced by the available data. In this paper, we therefore derive the model-based risk measures TTCE, Gaussian method and survival analysis and compare them in simulations with

Copyright © 2018 Society of Automotive Engineers of Japan, Inc. All rights reserved

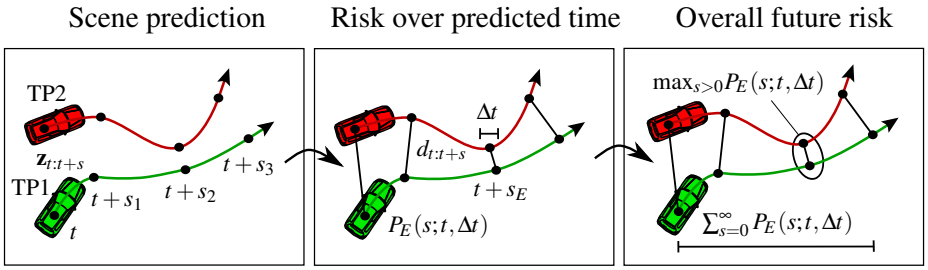


Fig. 1. General approach for collision risk prediction of two traffic participants.

the purpose of analyzing their properties for an application to ADAS and AD. Each measure is a representative of a broader family [8,9,12] and has been enhanced so that they can deal with temporal and spatial uncertainties. The depicted results are based on a conference paper published in FAST-zero 2017. [13] In the next Section 2, we outline the properties of a suitable risk measure and the general steps for its computation. Section 3 gives a detailed introduction of the three chosen risk measures and in Section 4 we show their performance and robustness on a set of longitudinal and intersection scenarios. Finally, in Section 5 we discuss future possible research areas.

2. Requirements and Framework

As a starting point, we consider dynamic collision scenarios (i.e. a traffic scene with two traffic participants TP1, TP2) at an arbitrary moment in time t. Beginning at t, the target is to estimate the risk of a critical event that could happen at a future time $t+s$, that is at a temporal distance s into the future. We assume the events to be disruptive and to have no duration, so that they can be fully characterized by their time $t+s$, if they happen at s into the future.

Since most of the commonly used risk measures do not address severity explicitly, we will concentrate on risk as an event occurrence probability. However, severity can be included into the argumentation in a straightforward way. An indicator for risk is then the probability function $P_E(s;t,\Delta t)$ that a critical event will happen during an interval of size Δt around a future time $t+s$. As a probability it should be positive and appropriately normalized, so that $P_E(s;t,\Delta t) \in [0,1]$. With a collision of time t_E (time *until* a collision occurs s_E), if a collision is imminent (at $s_E \to 0$), it should be $\lim_{s\to 0} P_E(s;t,\Delta t) \to 1$ and if no collision ever occurs, it should be $\lim_{s\to\infty} P_E(s;t,\Delta t) \to 0$.

A compact risk measure $R(t)$ would comprise, for each point in time t, the entire **accumulated expected future risk** contained in $P_E(s;t,\Delta t)$, $s \in [0,\infty]$. There are several possible ways to gain such a measure, e.g. by extracting the maximal expected risk

$$R(t) := \max_{s>0} P_E(s;t,\Delta t) \qquad (1)$$

or using an appropriatedly accumulated risk

$$R(t) := \sum_{s=0}^{\infty} P_E(s;t,\Delta t) \ . \qquad (2)$$

The latter is a cleaner form because it comprises the full future event probability, but it requires a more careful derivation due to proper normalization considerations. Additionally, heuristically motivated risk measures often directly estimate $R(t)$ without $P_E(s;t,\Delta t)$ (see Section 3.1). Again here, it should be guaranteed that $R(t) \in [0,1]$ and $R(t) \to 1$ for collision at $s_E \to 0$ and $R(t) < 1$ for no collision at any time.

A risk estimation framework consists of three components as depicted in Fig. 1. In a first step, a prediction of how the situation will evolve in the future is performed. In our notation, designating $\mathbf{z}$ as the state vector of a scene, the predicted sequence of future scene states is given by $\mathbf{z}_{t:t+s}$. The prediction can thereby be modeled at different levels of detail depending on the geometry, kinematics and interaction. For example, a low-level prediction would treat vehicles as dynamic entities and use constant acceleration, velocity or turn-rate assumptions in kinematic equations. On a next level, road geometries could be taken into account to constrain the paths on which vehicles can drive. The outcome of the prediction is a selected set of possible future trajectories for each involved vehicle.

In a second step, the time evolution of the scene $\mathbf{z}_{t:t+s}$ is evaluated in terms of criticality by extracting features which are indicative of risk. For collision risk, the predicted trajectories are compared for each point in predicted time s to obtain the spatiotemporal proximity $d_{t:t+s}$ between the vehicle trajectories. This leads to an **instantaneous risk** function or in features like the time to and distance at the point of maximal risk, resp. the time until the event s_E and the predicted proximity d_{t+s_E} at that time. Afterwards, the event probability $P_E(s;t,\Delta t)$ can be calculated from the instantaneous risk function. The third step comprises retrieving the risk measure in form of a scalar risk function $R(t)$ according to Eq. (1) or (2).

3. Theory of Risk Measures

3.1. Time-To-Closest-Encounter (TTCE)

The family of TTX-based risk measures are proximal safety indicators based on the time left until a critical event. In particular, the well-known TTC represents the time remaining until two vehicles will engage in a collision if they continue driving along the same path according to some prediction model [5]. A usual assumption is that both TP's drive with constant longitudinal velocities $v_{1,2}$. In this case, if they start driving at t with longitudinal positions $l_{1,2}$, the time of collision / time of critical event will be at $s_E = \mathrm{TTC} = -\Delta l/\Delta v$, with $\Delta l := l_1 - l_2$ and $\Delta v = v_1 - v_2$. However, TTC is rather limited for complex scenes, because (i) it is only applicable to longitudinal resp. 1D scenarios and (ii) it presumes that a collision will happen with certainty, so that near-crash cases cannot be evaluated. Several extensions of TTC to 2D have been developed [7], but generally lack justification both from theoretical as well as from empirical side.

For deriving a risk measure with TTC, the heuristic assumption is made that the overall risk of a predicted collision at a time s_E into the future decreases with increasing tempo-

Copyright © 2018 Society of Automotive Engineers of Japan, Inc. All rights reserved

ral distance to the event if nothing changes. When there is more time left until the incident, there is a larger chance for other things to happen (either voluntarily or unvoluntarily) which might lead to a different future evolution of the scene and to an avoidance of the event. An in-depth explanation is described later in Section 3.3. The most straightforward approach is then to calculate s_E in order to get $R(t)$ according to

$$R_{\mathrm{TTC}}(t) \sim \left[\frac{1}{s_E}\right]^{\alpha} \tag{3}$$

with $\alpha > 0$. To avoid divergence and to fulfill the normalization conditions from Section 2 we introduce a small constant ε and a steepness constant D_c so as to retrieve

$$R_{\mathrm{TTC}}(t) := \left[\frac{\varepsilon}{\varepsilon + D_c\, s_E}\right]^{\alpha} . \tag{4}$$

3.1.1. Extension for 2D operation

Critical events like passing-by at high velocity can not be captured by Eq. (4). A logical refinement is given by considering not only collision events, but generally the future events of highest criticality as a temporal reference. In case of collision risk, this leads to the time of closest proximity $s_E = \mathrm{TTCE}$. We moreover separate the TTCE-dependent risk into two factors: One that handles the temporal decay in the usual way and another one that accounts for the increased spatial collision danger in case of high proximity. In this way, we obtain

$$R_{\mathrm{TTCE}}(t) := \left(\frac{\varepsilon}{\varepsilon + D_c\, s_E}\right)^{\alpha} \exp\left\{-\frac{d_E^2}{2\sigma^2}\right\} \tag{5}$$

with the Euclidean distance $d_E := d(t + s_E)$ between the vehicles at the moment of the critical event and a Gaussian variance σ^2.

In case of a collision, we would retain $d_E = 0$ and the spatial term reduces to 1, so that we get back to $R_{\mathrm{TTC}}(t)$. In case of a near-crash incident, the spatial term can be used to quantify how critical the incident was in terms of spatial proximity, accounting for uncertainty in the predicted positions. As a further modification, we model the fact that spatial uncertainty in the predicted positions increases with larger prediction times s_E (see also Section 3.2). This means that for events which lie further away in the future, we will consider larger σ's with $\sigma(t + s_E) := D_c\, s_E$, so that

$$R_{\mathrm{TTCE}}(t) := \underbrace{\left(\frac{\varepsilon}{\varepsilon + D_c\, s_E}\right)^{\alpha}}_{\text{temporal uncertainty}} \underbrace{\exp\left\{-\frac{d_E^2}{2D_c\, s_E}\right\}}_{\text{spatial uncertainty}} . \tag{6}$$

With a prediction model for the trajectories $\mathbf{x}_{1,2}(t+s)$ of two TP's, we can directly calculate $s_E = \mathrm{TTCE}$ as well as d_E at that time. In case of constant velocity assumptions

$$\mathbf{x}_{1,2}(t+s) = \mathbf{x}_{1,2}(t) + \mathbf{v}_{1,2}\, s \tag{7}$$

we gain

$$\begin{aligned} d(t+s) &= \|\Delta\mathbf{x}(t) + \Delta\mathbf{v}\, s\| \\ &= \sqrt{[\Delta\mathbf{x}(t)]^2 + 2\Delta\mathbf{x}\Delta\mathbf{v}\, s + (\Delta\mathbf{v})^2 s^2} \end{aligned} \tag{8}$$

which has its minimum at

$$s_E = -\frac{\Delta\mathbf{x}(t)\,\Delta\mathbf{v}}{\|\Delta\mathbf{v}\|^2} \tag{9}$$

and which reduces to TTC in the longitudinal case. The distance of closest proximity is finally

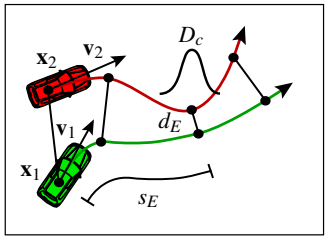


Fig. 2. Collision risk prediction with TTCE.

$$\begin{aligned} d_E &= \sqrt{[\Delta\mathbf{x}(t) + \Delta\mathbf{v}\, s_E]^2} \\ &= \sqrt{\left\{\Delta\mathbf{x}(t) - \frac{\Delta\mathbf{v}\,[\Delta\mathbf{x}(t)\,\Delta\mathbf{v}]}{\|\Delta\mathbf{v}\|^2}\right\}^2} \\ &= \sqrt{\left[\frac{(\Delta\mathbf{x}(t)\times\Delta\mathbf{v})\times\Delta\mathbf{v}}{\|\Delta\mathbf{v}\|^2}\right]^2} \\ &= \|\Delta\mathbf{x}(t)\|\,|\sin[\angle(\Delta\mathbf{x}(t),\Delta\mathbf{v}]|. \end{aligned} \tag{10}$$

As a result, using d_E from Eq. (10) and inserting it into the spatial term of Eq. (6) we have gained a risk measure which generalizes TTC to the 2D as well as to non-collision cases. Fig. 2 summarizes TTCE and its main variables.

3.2. Gaussian Method

As a second family of collision risk indicators, we consider approaches based on spatial occupancy probabilities [(1)]. For this purpose, the normalized probability densities for the respective spatial positions of two TP's indexed 1,2 are described by Gaussian functions

$$f_{1,2}(x) = \frac{1}{\sqrt{2\pi\sigma_{1,2}^2}} \exp\left[-\frac{(x-\mu_{1,2})^2}{2\sigma_{1,2}^2}\right] \tag{11}$$

with the mean positions $\mu_{1,2}$ and variances $\sigma_{1,2}$. [1]

A collision at a position x then occurs if *both* TP's coincide at the same position. Consequently, a way to quantify the likelihood of a coincidence/collision at a common position x is

$$f_c(x) := f_1(x) f_2(x) \ . \tag{12}$$

Because the product of two Gaussians is again a (non-normalized) Gaussian function, we get

$$f_c(x) = \frac{S_c}{\sqrt{2\pi\sigma_c^2}} \exp\left[-\frac{(x-\mu_c)^2}{2\sigma_c^2}\right] \tag{13}$$

with

$$\frac{1}{\sigma_c^2} = \frac{1}{\sigma_1^2} + \frac{1}{\sigma_2^2}, \tag{14}$$

$$\mu_c = \frac{\mu_1\sigma_1^2 + \mu_2\sigma_2^2}{\sigma_1^2 + \sigma_2^2} \quad \text{and} \tag{15}$$

$$S_c = \frac{1}{\sqrt{2\pi(\sigma_1^2 + \sigma_2^2)}} \exp\left[-\frac{(\mu_1-\mu_2)^2}{2(\sigma_1^2+\sigma_2^2)}\right]. \tag{16}$$

The Gaussian position probability densities encompass the final positions of all possible trajectories that lead to points x at a certain moment in time $t + s$. The probability that the first TP, driving along its trajectory, is hit by the

[1] For simplicity, we consider here the isotropic 1D case, but extensions to 2D and orientation are straightforward.

Copyright © 2018 Society of Automotive Engineers of Japan, Inc. All rights reserved

second TP is eventually given by spatially integrating $f_c(x)$ over all positions where the first TP can be

$$P_E(s;t,\Delta t) \sim \int_{\infty} f_c(x)\,dx = S_c \quad . \tag{17}$$

3.2.1. From Collision Probability to Risk Measure

So how do we get from the collision probability factor (17) to a risk measure as a function of the time t as introduced in Eq. (6)? First, we assume the moving TP's to follow a trajectory which undergoes certain variations in speed and heading. This accounts for mean positions through time $\mu_{1,2}(t+s)$ with spatial uncertainties $\sigma_{1,2}(t+s)$. For $\sigma_{1,2}(t+s)$ a simple Brownian motion diffusion model with a linear increase of uncertainty starting at $\sigma_{1,2}(t)=0$ is used according to

$$\sigma_{1,2}^2(t+s) := D_{1,2}\,s. \tag{18}$$

When we put Eq. (18) into (17), we obtain

$$P_E(s;t,\Delta t) \sim \frac{1}{\sqrt{2\pi D_c\,s}} \exp\left\{-\frac{[d(t+s)]^2}{2D_c\,s}\right\} \tag{19}$$

with a joint diffusion constant $D_c := D_1 + D_2$ and an "expected" distance $d(t+s) := \|\mu_1(t+s) - \mu_2(t+s)\|$. Furthermore, to satisfy the requirements of Section 2 we add a small constant ε to the first term and thus gain

$$P_E(s;t,\Delta t) := \left(\frac{\varepsilon}{\varepsilon + D_c\,s}\right)^{\alpha} \exp\left\{-\frac{[d(t+s)]^2}{2D_c\,s}\right\} \tag{20}$$

with $\alpha = 1/2$.

Eq. (20) describes the probability that two TP's will be at the same position within a future interval around $[t+s]$, starting at t and assuming Gaussian distributed positions around the TP's mean positions $\mu_{1,2}$. It can be seen that for larger prediction horizons s the overall collision likelihood decreases, because of the larger uncertainty in the TP's positions. The square-root dependency $\alpha = 1/2$ is hereby a direct consequence of the Gaussian approach and the diffusion spread of the spatial probability densities. However, in a scene with allowed and non-allowed areas (road / non-road) every time a TP leaves the road area it will already deviate from its "normal" prediction, so that the collision probability will exhibit a faster decay with s.

From Eq. (20) we can now distill a risk measure. As a conservative approach, we extract the maximal encountered future event probability as a risk indicator with

$$s_E := \mathrm{argmax}_s\, P_E(s;t,\Delta t) \tag{21}$$

and retrieve for the Gaussian risk indicator

$$R_{\mathrm{Gauss}}(t) := P_E(s_E;t,\Delta t) \tag{22}$$

or rather

$$R_{\mathrm{Gauss}}(t) := \left(\frac{\varepsilon}{\varepsilon + D_c\,s_E}\right)^{\alpha} \exp\left\{-\frac{d_E^2}{2\sigma^2}\right\} \tag{23}$$

whereas d_E is again the Euclidean distance at the moment of the critical event $d_E = d(t+s_E)$.

In Fig. 3, the increasing Gaussian position distributions are pictured, whereas the overlap between both at the closest distance d_E is taken for $R_{\mathrm{Gauss}}(t)$. Eq. (23) has the same form as Eq. (6). The difference is in the calculation of s_E, which in Section 3.1 occurs directly with TTCE, whereas here we estimate it via the maximized $P_E(s;t,\Delta t)$. For small diffusion constants $D_c \to 0$ or imminent collisions $s_E \to 0$, the two approaches become equivalent.

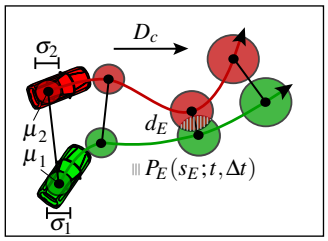


Fig. 3. Collision risk prediction with Gaussian method.

3.3. Survival Analysis

In Sections 3.1 and 3.2, we have seen two extensions of standard risk measures which try to circumvent some of their deficits. In particular, dealing with uncertainty over time and space as well as a generalization to 2D enables the use of risk measures in a broader range of situations. However, neither TTCE nor the Gaussian method provide a solid theoretical explanation, but rather motivated heuristics. In this Section, we describe a risk measure based on a grounded approach for the statistics of rare events and first passage time problems. This risk measure is also able to deal with uncertainties, but differently to the previously presented ones it provides full interpretability in terms of (normalized) probabilities and it considers additionally the situation history.

Accident occurrences are modeled as a thresholding process based on a Poisson-like event probability [12]. For an exemplary vehicle, in a sufficiently small time interval of size Δt the so-called **instantaneous event probability** is characterized by an **event rate** $\hat{\tau}^{-1}$ (units: events/sec) according to

$$\hat{I}_{\mathrm{event}}(\Delta t) := \hat{\tau}^{-1}\Delta t \quad . \tag{24}$$

The term *instantaneous* event probability denotes the fact that this probability does not (yet) take the history into account.

The **survival probability** function $\hat{S}(t+s;t)$ indicates the probability that the vehicle will survive from t until $t+s$, i.e. that it will not be engaged in an event like an accident. From Eq. (24), we can directly derive the survival probability after a small time interval Δt if the survival probability at t' was $\hat{S}(t';t)$

$$\hat{S}(t'+\Delta t;t) = \hat{S}(t';t)\,[1 - \hat{\tau}^{-1}\Delta t] \tag{25}$$

so that with the starting condition $\hat{S}(t;t)=1$ we get

$$\hat{S}(t+s;t) = \exp\{-\hat{\tau}^{-1}s\} \tag{26}$$

which describes the **homogeneous survival probability** for constant $\hat{\tau}^{-1}$.

The real risk event modeling occurs by a proper parameterization and variation of the time-varying $\hat{\tau}^{-1}(t)$ resp. its state-dependent analogous function $\tau^{-1}(\mathbf{z}_t)$ with $\hat{\tau}^{-1}(t) = \tau^{-1}(\mathbf{z}_t)$. In $\tau^{-1}(\mathbf{z}_t)$, we include all the risk factors with the context information in the state vector $\mathbf{z}_t$. Correspondingly, in dangerous situations the event rate will be higher than in harmless situations. For temporally varying $\hat{\tau}^{-1}(t)$, Eq. (26) modifies to

$$\hat{S}(t+s;t) = \exp\{-\int_o^s \hat{\tau}^{-1}(t+s')\,ds'\} \quad . \tag{27}$$

The states have been left out here for simplicity of the derivations. If we include them back, we acquire the state-dependent survival probability function

Copyright © 2018 Society of Automotive Engineers of Japan, Inc. All rights reserved

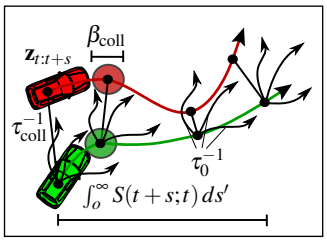


Fig. 4. Collision risk prediction with survival analysis.

$$S(t+s;t,\mathbf{z}_{t:t+s}) = \exp\{-\int_o^s \tau^{-1}(\mathbf{z}_{t+s'})\,ds'\} \qquad (28)$$

which defines the probability that a vehicle survives during $[t,t+s]$ without being involved in a critial event and which depends on the entire state vector sequence $\mathbf{z}_{t:t+s}$.

3.3.1. From Survival Probability to Risk Measure

To quantify the risk of an accident between the ego-car and another car, the (time-varying!) **spatial risk instantaneous collision event rate** $\tau_c^{-1}(\mathbf{z})$ is modelled by

$$\tau_{\text{coll}}^{-1}(\mathbf{z}) = \tau_{\text{coll},0}^{-1}\, e^{-\beta_{coll}\,|\mathbf{x}_1-\mathbf{x}_2|} \qquad (29)$$

with constants $\tau_{\text{coll},0}^{-1}$ and β_{coll}. While the scale factor $\tau_{\text{coll},0}^{-1}$ is chosen so that $\hat{I}_{\text{event}}(\Delta t,\mathbf{z})$ of each other car approaches 1 at collision, the steepness factor β_{coll} is used to model the position uncertainty originated from several possible sources like sensor inaccuracy, state prediction errors, unexpected driver behavior or unknown vehicle sizes. With β_{coll}, closer proximity leads to higher $\tau_{\text{coll}}^{-1}(\mathbf{z})$ and accordingly to a reduced probability of "surviving".

The approach is consistently extensible to different types and sources of risk by using a composed event rate like

$$\begin{aligned}\tau^{-1}(\mathbf{z}) &:= \tau_0^{-1} + \tau_{\text{coll}}^{-1}(\mathbf{z}) + \tau_{\text{ctrl}}^{-1}(\mathbf{z}) + \ldots \\ &= \tau_0^{-1} + \tau_{\text{crit}}^{-1}(\mathbf{z}) \end{aligned} \qquad (30)$$

which can comprise the terms related to critical events, such as vehicle-to-vehicle collisions τ_{coll}^{-1}, losing control in curves τ_{ctrl}^{-1} and others. The **escape rate** τ_0^{-1} plays a special role: It contains all (unknown and non-critical) "escape" events which might lead to the case that the currently predicted future gets invalid and later critical events lying further away in the future cannot occur any more. For instance, if we assume constant velocity in the prediction and the collision will occur at TTC = 10s, each disturbance, voluntary or involuntary action away from the constant velocity assumptions that occurs within $[t,t+\text{TTC}]$ will prevent the collision to happen (the driver will "escape" from the collision).

By multiplying the instantaneous event probability from Eq. (24) with the survival probability from Eq. (28), the **event probability** can be calculated as

$$E(s;t,\Delta t,\mathbf{z}_{t:t+s}) = I_{\text{event}}(\Delta t,\mathbf{z}_{t+s})\,S(t+s;t,\mathbf{z}_{t:t+s}). \qquad (31)$$

This is the probability that any type of event (escape event or critical) will happen in an interval of length Δt around $t+s$, given a state vector history $\mathbf{z}_{t:t+s}$ if we start observations at t and no event happened during $[t,t+s]$. Correspondingly, the **event density** (i.e. the probability of events per time unit) after a time s starting at t is given by

$$\begin{aligned} e(t+s;t,\mathbf{z}_{t:t+s}) &:= E(s;t,\Delta t,\mathbf{z}_{t:t+s})/\Delta t \\ &= \tau^{-1}(\mathbf{z}_{t+s})\,S(t+s;t,\mathbf{z}_{t:t+s}) \end{aligned} \qquad (32)$$

and the total **time-accumulated event probability** (i.e. the probability that any of the events will happen during $[t,t+s]$) by

$$A(s;t,\mathbf{z}_{t:t+s}) := \int_o^s e(s';t,\mathbf{z}_{t:t+s'})\,ds' \ . \qquad (33)$$

As a risk measure, we want to take the time-accumulated probability of the critical events only. If we separate the critical events from the escape events (which "avoid" the accidents), we find out that the event density

$$\begin{aligned} e(s;t,\mathbf{z}_{t:t+s}) &= \tau^{-1}(\mathbf{z}_{t+s})\,S(t+s;t,\mathbf{z}_{t:t+s}) \\ &= [\tau_0^{-1} + \tau_{\text{crit}}^{-1}(\mathbf{z}_{t+s})]\,S(t+s;t,\mathbf{z}_{t:t+s}) \\ &:= e_0(s;t,\mathbf{z}_{t:t+s}) + e_{\text{crit}}(s;t,\mathbf{z}_{t:t+s}) \end{aligned} \qquad (34)$$

also separates into two respective terms. Consequently, for the time-accumulated event probability

$$A(s;t,\mathbf{z}_{t:t+s}) = A_0(s;t,\mathbf{z}_{t:t+s}) + A_{\text{crit}}(s;t,\mathbf{z}_{t:t+s}) \ . \qquad (35)$$

holds true. The first term quantifies the overall future probability that critical events will be avoided during $[t,t+s]$, whereas the second term expresses the future probability of getting involved in a critical event during the same time span.

Since we are interested in the estimation of the time-accumulated future risk, we use

$$P_E(s;t,\Delta t) := e_{\text{crit}}(s;t,\mathbf{z}_{t:t+s})\Delta t \qquad (36)$$

as our time-resolved differential risk measure. The integral risk measure then is

$$R(t) = A_{\text{crit}}(\infty;t,\mathbf{z}_{t:t+\infty}) \qquad (37)$$

It can be shown that the time-accumulated event probability integrates to 1, which means

$$A(\infty;t,\mathbf{z}_{t:t+\infty}) = 1 \ . \qquad (38)$$

This is a sensible and necessary normalization condition, because for an infinite future a critical event will happen with certainty 1.

Using this information, we arrive at

$$R_{\text{SA}}(t) = 1 - A_0(\infty;t,\mathbf{z}_{t:t+\infty}) \qquad (39)$$

$$= 1 - \underbrace{\tau_0^{-1}\int_o^\infty S(t+s;t,\mathbf{z}_{t:t+s'})\,ds'}_{\text{Overall escape probability}} \qquad (40)$$

for our final risk measure. It contains the overall probability of escaping a future critical event and its complement quantifies the overall probability of engaging in a future critical event. Besides, it is well-behaved in the limiting cases. The risk measure automatically approaches 0 if there are no critical events present, since then the overall escape probability approaches 1 and for an imminent critical event, the escape probability reaches 0 as there is no time left for any type of escape events in terms of avoidance behavior or similar. Fig. 4 illustrates τ_0^{-1} as trajectory alternatives changing $\mathbf{z}_{t:t+s}$, the positional uncertainty β_{coll} and the procedure of integrating the survival function $S(t+s;t)$ over the predicted time s which among others depends on τ_{coll}^{-1}.

4. Simulation Results

4.1. Evaluation of Single Longitudinal and Intersection Scenario

For a quantitative comparison, we applied the presented three risk measures to real crash cases taken from the German In-Depth Accident Study (GIDAS) dataset [14]. The GIDAS Pre-Crash-Matrix contains reconstructed trajectories of

Copyright © 2018 Society of Automotive Engineers of Japan, Inc. All rights reserved

two TP's involved in an upcoming collision for longitudinal and intersection scenarios on average t = -5.5 s ahead. In order to also quantify the risk for near-crash cases, we additionally changed the course of the scene evolution. In the longitudinal car-following example, the path of one TP was shifted laterally in such a way that the minimal distance is $d_E = 7\,\mathrm{m}$ instead of $d_E = 0\,\mathrm{m}$. There is no collision anymore, but a close passing. In the intersection example, we used for one TP the Foresighted Driver Model (FDM) [15], which changes the velocity profile $v(t)$ of its trajectory. Accordingly, the TP decelerates and lets the other TP pass to avoid an accident.

At every timestep t in the simulation, a constant velocity model is used for both TP's to predict the distance $d_{t:t+s}$ for future times s. The prediction horizon is set as $s_H > 5.5\,\mathrm{s}$ so that the time of crash or near-crash s_E is within the prediction interval. The sequence $d_{t:t+s}$ represents the input for all three risk measures. In this way, they have the same prerequisites and if the real trajectory violates the constant velocity assumption with an acceleration $a(t) \neq 0\,\mathrm{m/s^2}$, all risk measures are equally impacted. Furthermore, we selected the parameter D_c of TTCE and the Gaussian method and τ_0^{-1} as well as β_{coll} for the survival analysis such that for the maximal risk value of each $R_{max} > 0.5$ holds true in the near-crash case.

Fig. 5 shows the simulation view of a longitudinal crash and near-crash case starting from time t = -5.3 s until the point of maximal criticalty $t_E = 0\,\mathrm{s}$ and plots of the risk measures $R_{\mathrm{TTCE}}(t)$, $R_{\mathrm{Gauss}}(t)$ and $R_{\mathrm{SA}}(t)$. Equally, Fig. 6 summarizes the simulation results for an intersection scenario with the interval $t = [\text{-}5.2\,\mathrm{s}, 0\,\mathrm{s}]$. In both scenarios $R_{\mathrm{SA}}(t)$ approaches 1 faster in the crash case and has a lower R_{max} in the near-crash case. Compared to $R_{\mathrm{TTCE}}(t)$, the performance of $R_{\mathrm{Gauss}}(t)$ is higher, but its robustness lower. The reason lies in the square-root dependency $\alpha = 1/2$ in $R_{\mathrm{Gauss}}(t)$ as opposed to $\alpha = 1$, which makes its curve shape flatter at $t < t_E$ and steeper close to t_E. Lastly, only for the longitudinal crash case $R_{\mathrm{TTC}}(t)$ can be calculated with the help of Eq. (4). It resembles $R_{\mathrm{TTCE}}(t)$, but has slightly higher values because of the missing spatial uncertainty term from Eq. (6).

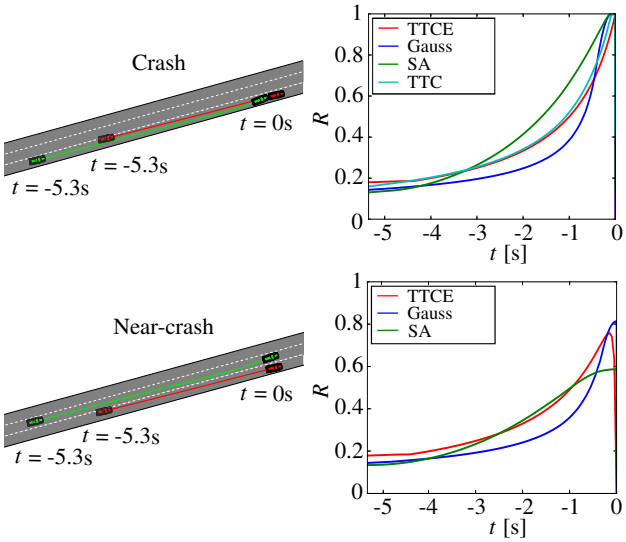


Fig. 5. Comparison of risk measures for longitudinal scenario with simulation view and their respective curves. Top: Crash case. Bottom: Near-crash case.

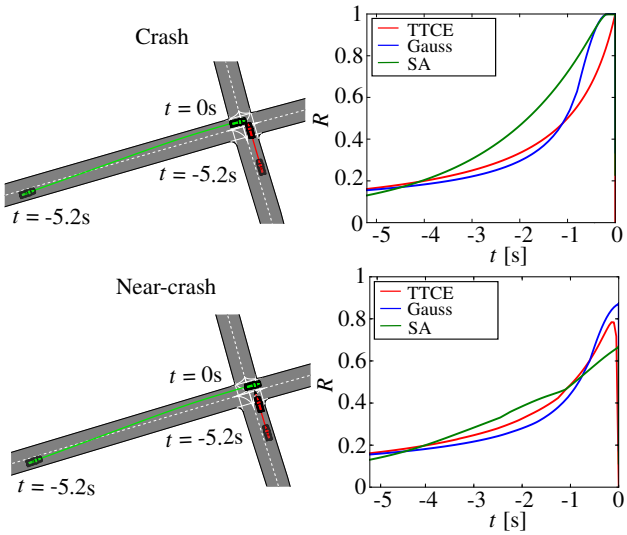


Fig. 6. Comparison of risk measures for intersection scenario.

4.2. Statistical Analysis for Multiple Scenarios

After demonstrating the general behavior of the risk measures, we now test them on a set of 42 scenarios. The set consists of 7 longitudinal and 7 intersection scenarios from GIDAS, which have not only a crash and near-crash case, but also a non-crash case. In the longitudinal example, we moved the path of one TP laterally so that $d_E = 12\,\mathrm{m}$ is reached and in the intersection samples, we set constant velocities for both TP with the result that they pass the intersection $|\Delta t| = 2s$ away from each other. In Fig. 7 the distance sequences $d(t)$ are pictured for all 42 test instances, which ranges from 120 m to 0 m. The pictured graphs $d(t)$ should not be confused with the predicted distances $d_{t:t+s}$, which are calculated at every time step t with the constant velocity model and which act as the input of the risk measures.

When a risk measure crosses a threshold of $R_{th} = 0.7$, we define it as having detected a crash. An optimal risk measure has an early detection time t_d of the crash in the crash cases and has no false-positive detections FP in the near- and non-crash cases, which occurs if $R_{max} > R_{th} = 0.7$ takes effect. In Table 1, the averaged values of t_d and R_{max} and the accumulated FP/N of each risk measure are listed for the 42 test samples. Furthermore, the variances σ_t and σ_R show the spread of the results. As anticipated from the last Section 4.1, the survival analysis has the highest $|t_d|$ and the lowest R_{max} and FP/N. The gaussian method exhibits a larger $|t_d|$ than TTCE, but in the near-crash case R_{max} and FP/N is smaller in TTCE. In general, a crash is detected later and there are more false detections in intersection compared to longitudinal scenarios. That is because a real trajectory with $a(t) \neq 0\,\mathrm{m/s^2}$ results into a more parabolic curve of $d(t)$ in intersection scenarios (see Fig. 7), which in turn causes higher errors in $d_{t:t+s}$ due to the constant velocity assumption. Finally, TTC is included as a standard method in the ADAS and AD community to measure collision risk. However, in the evaluated cases the performance of our developed three risk measures has proven to be better and

Copyright © 2018 Society of Automotive Engineers of Japan, Inc. All rights reserved

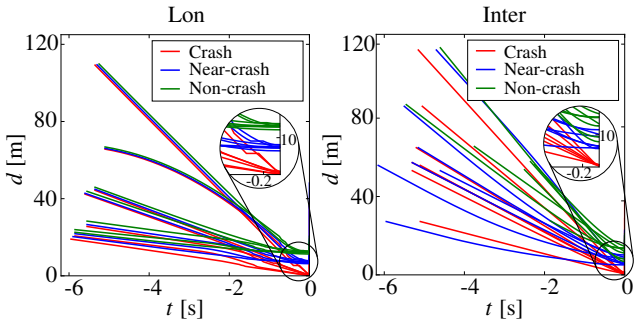


Fig. 7. Variance in distance sequences of extended GIDAS dataset. Left: Longitudinal scenario. Right: Intersection scenario.

they work in a broader range of scenarios, i.e. in intersection scenarios as well as in near- and non-crash cases. [2]

5. Discussion and Outlook

In this work, we first extended the heuristic risk measures TTC and Gaussian method to be able to deal with temporal and spatial uncertainty and to fulfill the normalization requirements for a general framework of collision risk prediction. For TTC, we additionally derived a 2D version called TTCE. In a second step, we introduced a theoretically justified survival analysis which separates events into critical and escape events and calculates a risk measure by integrating the probability to survive over the predicted time. Each of the three methods precede a prediction step of the scene evolution with the output of predicted distances.

In simulations of longitudinal and intersection scenarios, the survival analysis resulted in having the highest performance in terms of early detection time in the crash cases as well as robustness with less false-positive detections in the near- and non-crash cases. The Gaussian method and TTCE have similar accuracy, which is reasonable since their underlying equations could be shown to be also very similar. Furthermore, both can be seen as an approximation of the survival analysis without history consideration.

Procedures to validate ADAS and AD have to be developed beyond existing safety tests driving millions of miles [(16)]. Since TTC only works for longitudinal scenarios and has moderate performance, the survival analysis is more suitable. In future work, we want to develop a risk indicator quantifying the entire experienced risk for long test drives and arbitrary driving situations.

Many motion planning methods act on TTC-based risk measures. Enhancements have been made in the FDM [(14)], which uses gradient descent on a modified TTCE with predicted trajectories from a constant velocity model. As an alternative, the survival analysis could be employed on multiple trajectories of arbitrary velocity profiles. The trajectory with the lowest risk is eventually chosen as the planned behavior. Such an approach that relies on sampling shows to be promising and needs to be examined.

[2] Remark: In Table 1, TTC has a higher (meaning better) $|t_d|$ compared to TTCE. This might seem unexpected, because we derived TTCE to be a generalization of TTC. However, the TTCE parametrization was optimized to work in all cases (crash, near-crash and non-crash), whereas the TTC implementation specializes on longitudinal crash cases only.

Table 1.
Statistics of risk measures for extended GIDAS dataset.

		Crash		Near-crash		Non-crash	
		Lon	Inter	Lon	Inter	Lon	Inter
TTCE	t_d [s]	-0.47	-0.45	–	–	–	–
	σ_t [s]	0.05	0.01	–	–	–	–
	R_{max}	–	–	0.78	0.75	0.62	0.63
	σ_R	–	–	0.02	0.08	0.01	0.08
	FP/N	–	–	7/7	4/7	0/7	2/7
Gauss	t_d [s]	-1.36	-0.85	–	–	–	–
	σ_t [s]	0.75	0.39	–	–	–	–
	R_{max}	–	–	0.84	0.82	0.53	0.57
	σ_R	–	–	0.03	0.11	0.03	0.16
	FP/N	–	–	7/7	6/7	0/7	2/7
SA	t_d [s]	-1.46	-1.14	–	–	–	–
	σ_t [s]	0.48	0.23	–	–	–	–
	R_{max}	–	–	0.63	0.63	0.35	0.42
	σ_R	–	–	0.04	0.12	0.02	0.15
	FP/N	–	–	0/7	3/7	0/7	0/7
TTC	t_d [s]	-0.76	–	–	–	–	–
	σ_t [s]	0.16	–	–	–	–	–

At last, it is possible to improve the collision risk estimation in general by separating the distance calculation into longitudinal and lateral components along the ego path and weighting the components differently. From our simulation experiences, we expect that this will render the method more sensitive yet further reducing the number of false positives in near-crash cases.

Acknowledgments

This work has been supported by the European Unions Horizon 2020 project *VI-DAS*, under the grant agreement number 690772.

References

(1) US Department of Homeland Security: Risk Management Fundamentals, pp. 19-21 (2011).

(2) S. Lefevre, D. Vasquez, and C. Laugier: A Survey on Motion Prediction and Risk Assessment for Intelligent Vehicles, Robomech Journal, Volume 1, Issue 1, pp. 1-14 (2014).

(3) M. Bojarski, D. Del Testa, D. Dworakowski, B. Firner, and et al.: End to End Learning for Self-Driving Cars, Computing Research Repository, abs/1604.07316 (2016).

(4) S. Klingelschmitt, M. Platho, H.-M. Gro, V. Willert, and J. Eggert: Combining Behavior and Situation Information for Reliably Estimating Multiple Intentions, Intelligent Vehicles Symposium, pp. 388-393 (2014).

(5) R. Van der Horst: Time-To-Collision as a Cue for Decision-Making in Braking, Vision in Vehicles III, pp. 19-26 (1991).

(6) H. Winner: Grundlagen, Komponenten, und Systeme fur aktive Sicherheit und Komfort, Handbuch Fahrerassistenzsysteme, pp. 522542 (2014).

(7) J. Ward, G. Agamennoni, S. Worrall, and E. Nebot: Vehicle Collision Probability Calculation for General Traffic Scenarios Under Uncertainty, Intelligent Vehicles Symposium, pp. 986-992 (2014).

(8) F. Damerow and J. Eggert: Predictive Risk Maps, Intelligent Transportation Systems Conference, pp. 703-710 (2014).

Copyright © 2018 Society of Automotive Engineers of Japan, Inc. All rights reserved

(9) S. Patil, J. Van den Berg, and R. Alterovitz: Estimating Probability of Collision for Safe Motion Planning under Gaussian Motion and Sensing Uncertainty, International Conference on Robotics and Automation, pp. 3238 - 3244 (2012).
(10) A. Lambert, D. Gruyer, and G. Saint Pierre: A fast Monte Carlo Algorithm for Collision Probability Estimation, Control, Automation, Robotics and Vision Conference, pp. 406-411 (2008).
(11) W. Wachenfeld, P. Junietz, R. Wenzel, and H. Winner: The Worst-Time-To-Collision Metric for Situation Identification, Intelligent Vehicles Symposium, pp. 729-734 (2016).
(12) J. Eggert: Predictive Risk Estimation for Intelligent ADAS Functions, Intelligent Transportation Systems Conference, pp. 711-718 (2014).
(13) J. Eggert and T. Puphal: Continuous Risk Measures for ADAS and AD, International Symposium on Future Active Safety Technology, (2017).
(14) C. Erbsmehl: Simulation of real crashes as a method for estimating the potential benefits of advanced safety technologies. In Technical Conference on the Enhanced Safety of Vehicles, No. 09-0162, (2009).
(15) J. Eggert, F. Damerow, and S. Klingelschmitt: The Foresighted Driver Model, Intelligent Vehicles Symposium, pp. 322-329 (2015).
(16) D. Zhao and H. Peng: From the Lab to the Street: Solving the Challenge of Accelerating Automated Vehicle Testing, Computing Research Repository, abs/1707.04792 (2017).

Copyright © 2018 Society of Automotive Engineers of Japan, Inc. All rights reserved